Electronic Phase Diagrams of Carriers in Self-Assembled Quantum Dots: Violation of Hund's Rule and the Aufbau Principle for Holes

Lixin He, Gabriel Bester, and Alex Zunger
National Renewable Energy Laboratory, Golden, Colorado 80401, USA
(Received 12 May 2005; published 9 December 2005)

We study the ground-state orbital and spin configurations of up to six electrons or holes loaded into self-assembled InAs/GaAs quantum dots. We use a general phase-diagram approach constructed from single-particle pseudopotential and many-particle configuration interaction methods. The predicted hole charging energies agree with recent charging experiments, but offer a different interpretation: we find that while the charging of *electrons* follows both Hund's rule and the Aufbau principle, the charging of *holes* follows a nontrivial charging pattern which violates both the Aufbau principle and Hund's rule.

DOI: 10.1103/PhysRevLett.95.246804 PACS numbers: 73.21.La, 73.23.Hk, 73.63.Kv

The remarkable combination of three-dimensional spatial confinement in quantum dots with the ability to integrate them into carrier-transporting device structures enables storage and retrieval of electrons [1–6], to the benefit of future quantum-computing [7,8], memory [9,10], and single-photon [11] applications. Unlike real atoms, where large Coulomb repulsion energies $J \simeq 10$ eV limit the number of stable ionized species to just a few, semiconductor quantum dots can be loaded by as many as six [1] to ten [12] electrons in colloidal [12] and self-assembled [1–3] dots, and up to hundreds of electrons in electrostatically confined dots [4–6]. Furthermore, one can measure for each ionization state the stable spin configuration [1,4–6], the energy to add another electron [1,2,4,5,12] as well as the attendant spectroscopic shifts with charging [3,13]. Like real atoms, the stable spin configuration observed in electrostatic dots [4–6], having lateral dimensions of 500–1000 Å, follow the rules of atomic physics; that is, the $s, p, d, \ldots$ shells are occupied in successive order with no holes left behind (Aufbau principle) and with maximum spin (Hund's rule). Recently, it became possible to load and measure electrons [1,2] and holes [2,14,15] into much smaller ($\simeq 200 \times 40$ Å), epitaxially grown self-assembled dots of InGaAs/GaAs. Electronic structure calculations for self-assembled dots [16] reveal that while for electrons the Coulomb energy $J_{ee} \simeq 20$ meV is *smaller* than the level spacing $\Delta\epsilon \simeq 50 - 70$ meV, for holes the Coulomb repulsion $J_{hh} \simeq 15 - 25$ meV is comparable to the level spacing $\Delta\epsilon \simeq 10 - 20$ meV. This opens the possibility of observing for holes some stable, exotic spin configurations that defy the rules of atomic physics. In this Letter, we apply a combination of an atomistic pseudopotential description [16] for the single-particle electronic structure, with a many-body configuration interaction (CI) description [17] of many-particle effects to both electron and hole loading into InGaAs/GaAs self-assembled quantum dots. We calculate the generalized electronic phase diagram of the system showing which many-particle configurations are energetically stable for various p-p and p-d splitting of the single-particle levels. We find that while *electron loading* follows both the Aufbau principle and Hund's rule, *hole loading* gives rise to stable but unusual spin configurations. While these calculated configurations agree with recent measurements [14,15], they differ from their interpretation [15], which assumes 2 dimensional (2D) parabolic models [18,19] that have been employed extensively to analyze very large electrostatically confined dots [4–6]. We show the reason for the failure of the simpler interpretation is that parabolic models ignore the interband and intervalley coupling existing in a real self-assembled quantum dot.

The "charging energy" $\mu(N)$ is the energy needed to add a carrier to the dot that is already charged by $N-1$ carriers: $\mu(N) = E(N) - E(N-1)$, where $E(N)$ is the correlated many-body total energy of the ground state of the N-particle dot. The "addition energy" $\Delta(N-1, N)$ (analogous to the difference between ionization potential and electron affinity) indicates how much more energy is needed to add the Nth carrier compared to the energy needed to add the $N-1$th carrier: $\Delta(N-1, N) = \mu(N) - \mu(N-1) = E(N) - 2E(N-1) + E(N-2)$. In the Hartree-Fock approximation, where the effect of correlations is neglected but the direct Coulomb and exchange interactions are retained, simple expressions can be derived for the addition energies. To do so, one needs to decide first what is the order of filling the single-particle $s, p, d, \cdots$ levels. Assuming the filling sequence of the left hand side of Fig. 1(a), (obeying Hund's rule and the Aufbau principle) and retaining only the diagonal interelectronic term as done in the current literatures on charging [19,20], the addition energies are given by

$$\begin{aligned}
\Delta_{\mathrm{HF}}(1,2) &= J_{ss}, \\
\Delta_{\mathrm{HF}}(2,3) &= (\epsilon_{p_1} - \epsilon_s) + 2J_{sp_1} - J_{ss} - K_{sp_1}, \\
\Delta_{\mathrm{HF}}(3,4) &= (\epsilon_{p_2} - \epsilon_{p_1}) + 2J_{sp_2} - 2J_{sp_1} \\
&\quad + J_{p_1p_2} - K_{sp_2} + K_{sp_1} - K_{p_1p_2}, \\
\Delta_{\mathrm{HF}}(4,5) &= (\epsilon_{p_1} - \epsilon_{p_2}) + 2J_{sp_1} - 2J_{sp_2} \\
&\quad + J_{p_1p_1} - K_{sp_1} + K_{sp_2} + K_{p_1p_2},
\end{aligned} \tag{1}$$

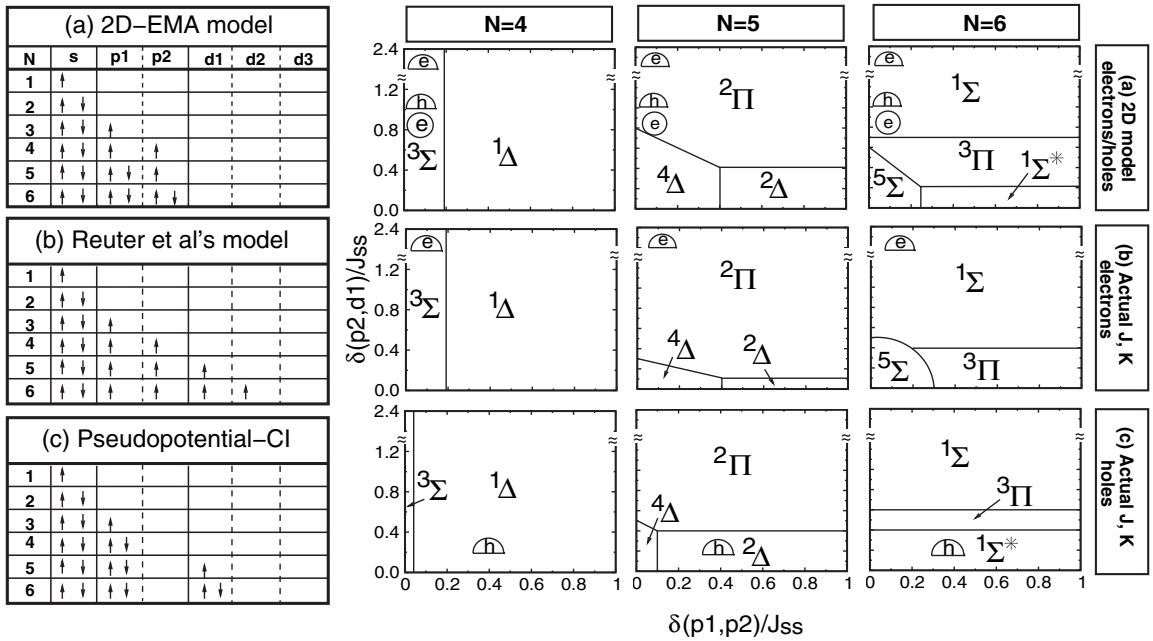

FIG. 1. (Left) The ground-state configurations (a) calculated from 2D parabolic model, (b) suggested by Reuter *et al* [15], and (c) calculated from pseudopotential-CI method. (Right) The phase-diagrams for $N = 4$, 5, 6 electrons and holes (a) calculated from 2D parabolic model, (b) for electrons using realistic Coulomb and exchange integrals, and (c) for holes using realistic Coulomb and exchange integrals. For $N = 6$, $\delta_{d_1,d_2} = \delta_{p_1,p_2}$ is assumed. Symbols denote the stablest configurations for specific dots: circles represent electrostatic dots, while lenses represent self-assembled dots. The configurations of phases are given by Eqs. (2)–(4).

where J_{ij} and K_{ij} are, respectively, the Coulomb and exchange integrals between states i and j.

To calculate the addition energy $\Delta(N-1, N)$, one must first construct a single-particle Schrödinger equation model. In this step, one might need to account not only for quantum confinement, but also for electronic structure effects such as multiband (light-hole, heavy-hole, conduction) coupling; intervalley (Γ-X-L) coupling; spin-orbit coupling; and the effect of strain and chemical intermixing. It is then possible to compute all of the single-particle level spacings and integrals entering Eq. (1), thus predict the value of $\Delta_{\mathrm{HF}}(N-1, N)$. Alternatively, one can neglect explicitly electronic structure effects other than quantum confinement, and use instead a particle-in-a-parabolic-box model, widely used in this field [18,19]. In this 2D effective mass approximation (EMA), the p levels are degenerate ($\epsilon_{p_1} = \epsilon_{p_2}$), as are the d levels ($\epsilon_{d_1} = \epsilon_{d_2} = \epsilon_{d_3}$) and the splitting between the s and p levels ($\varepsilon_s - \varepsilon_p$), and the splitting ($\varepsilon_p - \varepsilon_d$) between the p and d levels are both equal to the harmonic oscillator frequency ω. Furthermore, the assumed parabolicity assures that analytic formulas can be derived [19] for the Coulomb and exchange matrix elements that relate all integrals needed for the addition energies to the value of a single J_{ss}, for instance in Eq. (1), $2J_{sp} - J_{ss} - K_{sp} = J_{ss}/4$. Thus, universal results can be derived for electrons and holes as shown in the right hand side of Fig. 1(a), for $N = 4, 5, 6$. Since the restriction of the 2D-EMA model to degenerate p and d shells and to equidistant shells ($\epsilon_p - \epsilon_s = \epsilon_d - \epsilon_p$) might be rather stringent [21], we allow in Fig. 1(a) (right side) $\delta_{p_1,p_2} = \epsilon_{p_2} - \epsilon_{p_1}$ and $\delta_{p_2,d_1} = \epsilon_{d_1} - \epsilon_{p_2}$ to vary, calculating for each $\{N; \delta_{p_1,p_2}, \delta_{p_2,d_1}\}$ the configuration which minimizes the total energy. This gives a "phase diagram" as a function of the parameters δ_{p_1,p_2} and δ_{p_2,d_1} in the unit of J_{ss} as shown in Fig. 1(a) (right side) for particle number $N = 4, 5, 6$. The 2D-EMA model yields for $N = 4$ two electronic phases:

$$^3\Sigma = (s^\uparrow s^\downarrow)(p_1^\uparrow)(p_2^\uparrow); \qquad ^1\Delta = (s^\uparrow s^\downarrow)(p_1^\uparrow p_1^\downarrow). \tag{2}$$

For $N = 5$, it gives three phases:

$$^4\Delta = (s^\uparrow s^\downarrow)(p_1^\uparrow)(p_2^\uparrow)(d_1^\uparrow); \qquad ^2\Pi = (s^\uparrow s^\downarrow)(p_1^\uparrow p_1^\downarrow)(p_2^\uparrow);$$
$$^2\Delta = (s^\uparrow s^\downarrow)(p_1^\uparrow p_1^\downarrow)(d_1^\uparrow), \tag{3}$$

while for $N = 6$, it gives four phases:

$$^5\Sigma = (s^\uparrow s^\downarrow)(p_1^\uparrow)(p_2^\uparrow)(d_1^\uparrow)(d_2^\uparrow); \quad ^3\Pi = (s^\uparrow s^\downarrow)(p_1^\uparrow p_1^\downarrow)(p_2^\uparrow)(d_1^\uparrow);$$
$$^1\Sigma = (s^\uparrow s^\downarrow)(p_1^\uparrow p_1^\downarrow)(p_2^\uparrow p_2^\downarrow); \quad ^1\Sigma^* = (s^\uparrow s^\downarrow)(p_1^\uparrow p_1^\downarrow)(d_1^\uparrow d_1^\downarrow). \tag{4}$$

Here, we use a spectroscopic notation $^{2S+1}\Lambda$ for systems with cylindrical symmetry, where $S = \sum_i s_i$, $\Lambda = \sum_i l_i$, and i is the ith occupied level. To decide which of these phases is a ground state, we need to know in Fig. 1(a) (right side) the value of $\delta_{p1,p2}/J_{ss}$ and $\delta_{p2,d1}/J_{ss}$. For electrons in self-assembled dots, $\delta_{p2,d1} > 2J_{ss}$ [1,19]. For holes, $\delta_{p2,d1} = 1.17J_{ss}$ was determined from recent experiments [14,15] and $\delta_{p1,p2} = 0$ is assumed in 2D-EMA model. This places the phases $^3\Sigma$, $^2\Pi$, $^1\Sigma$, as ground states for $N = 4, 5, 6$, respectively, [Fig. 1(a) (right side)] for both electrons and holes. The ground-state configurations of the

2D-EMA model are collected in Fig. 1(a) (left side), for $N = 1 - 6$.

For *electrons*, the ground states of 2D-EMA model are corroborated by atomistic pseudopotential calculations [Fig. 1(b) (right side)], where we use the Coulomb integrals obtained from atomistic wave functions for electrons in a lens shape InAs/GaAs dot with 25 nm base and 2.5 nm height. This shape is realistic, according to experimental findings [23], and predicts a fundamental photoluminescence line very close to the one observed in the charging experiment [15] at around 1 eV. Overall, the comparison between Figs. 1(a) and 1(b) (right side) shows that while the phase boundaries can change significantly when realistic wave functions are assumed instead of 2D-EMA values, the ground-state symmetries for $N = 5$ and 6 electrons in self-assembled dots remain unchanged and are far from other competing phases.

The foregoing analysis of loading of *electrons* [4–6] has been simplified by the fact that the single-band effective mass model is not a drastic approximation given that in strongly direct-gap zinc-blende materials (e.g., InAs, InP) electrons derive from a nondegenerate, spin-orbit-free Γ_{1c} band which is energetically isolated from other states. The analysis of loading of *holes*, however, does not benefit from the same simplification, as holes derive from a mix of heavy- and light-hole states, invalidating [24] the classification of hole states as pure s or p or d levels and as pure heavy-hole or light-hole states [25]. Reuter *et al.* [15] used a 2D-EMA model to analyze their hole charging results. The value of J_{ss} is directly accessible from experiments since it is well approximated by $\Delta(1, 2)$ [Eq. (1)]. The only remaining parameter in the 2D-EMA model is the single-particle energy splitting $(\epsilon_s - \epsilon_p) = (\epsilon_p - \epsilon_d) \equiv \omega$ which can be extracted from measuring $\Delta(2, 3) = (\epsilon_p - \epsilon_s) + J_{ss}/4$. Reuter *et al.* [15] thus determined $J_{ss} = 23.9$ meV and $\varepsilon_p - \varepsilon_s = 28$ meV. Since experimentally five addition energies are available and only two were used in the fit above, the problem is overdetermined and it is possible to assess how well the model reproduces the remaining three experimental data points. Assuming $\delta_{p1,p2} = 0$ and $\delta_{p2,d1} = \epsilon_d - \epsilon_p = \epsilon_p - \epsilon_s = 28$ meV, yields the above mentioned $\delta_{p2,d1} = 1.17 J_{ss}$, leading to the phase diagram of Fig. 1(a) (right side), with ground-state phases $^3\Sigma$, $^2\Pi$, and $^1\Sigma$. If one calculates the addition energies of Eq. (1), using these ground-state configurations one gets the values indicated by "2D-EMA model ground state" in Table I. However, as noted by Rueter *et al.*, this hole addition sequence contradicts the magnetic field data [15], which show that the hole d levels are occupied before p levels are filled completely (non-Aufbau) [15]. To explain their magnetic field data, Reuter *et al.* [15] assumed a hole filling sequence [Fig. 1(b) (left side)] that relies on an *ad hoc* excited hole state instead of the ground states predicted by the 2D-EMA model [Fig. 1(a) (left side)]. In Table I, we compare the ensuing addition energies of both the ground-state and excited state configurations with experiments. We find that the addition energies given by both scenarios of Fig. 1(a) and 1(b) (left side) show significant discrepancies from the experimental values, with about 25–50% error.

The atomistic pseudopotential, plus CI calculations, show different ground-state configurations for holes than the above two models. In the CI calculations, we used all Slater determinants constructed from 16 single-particle levels (with spin). This gives 8008 configurations for 6 holes. The total energies are converged to about 1 meV. In a CI calculation, the ground states usually mix several different configurations, but the leading CI configurations have a significant weight, being 79%, 71%, and 64% for 4, 5, and 6 holes, respectively, in the 20×2.5 nm dot. In what follows, we will thus refer to a CI solution by denoting its leading configuration. As shown in Fig. 1(c) (right side), for $N = 4$, and $N = 5$, the topology of the phase diagrams are the same as in the 2D-EMA model, but the boundaries are shifted. As a result, for $N = 4$, the hole ground state is now phase $^1\Delta$ not $^3\Sigma$ and for $N = 5$, the ground state is phase $^2\Delta$ not $^2\Pi$. For $N = 6$, the topology of the phase diagram changed completely: phase $^5\Sigma$ disappeared, and the ground state is now $^1\Sigma^*$. The ground-state configurations are listed in Fig. 1(c) (left side) for $N = 1 - 6$ [25]. Using these new ground states, Table I compares the experimental addition energies and the calculated results for six different InAs/GaAs lens-shaped quantum dots of different bases and heights. Very good agreement is ob-

TABLE I. Hole addition energies of self-assembled InAs/GaAs quantum dots in meV. The experimental values are from Ref. [15] at zero magnetic field. The "ground-state" values correspond to the low-spin configurations as given in Fig. 1(a) (left side) and the "excited state" values to the high-spin configurations assumed in Ref. [15] and given in Fig. 1(b) (left side). The results of "pseudopotential + CI" calculations correspond to the configurations from Fig. 1(c) (left side). All sizes are in nm.

		2D-EMA model		Pseudopotential + CI					
Addition		Ground state	Excited state	$2R = 20$		$2R = 25$		$2R = 27.5$	
energy	Exp.	Figure1(a) (left)	Figure1(b) (left)	$h = 2.5$	$h = 3.5$	$h = 2.5$	$h = 3.5$	$h = 2.5$	$h = 3.5$
$\Delta_h(1, 2)$	23.9	Fitted	Fitted	24.1	19.0	21.9	17.5	21.0	16.7
$\Delta_h(2, 3)$	34.2	Fitted	Fitted	28.7	21.7	27.2	21.2	26.4	20.6
$\Delta_h(3, 4)$	17.1	12	12	18.1	16.9	16.4	15.2	15.6	14.5
$\Delta_h(4, 5)$	23.2	21	29	26.4	21.6	25.4	20.8	23.8	20.5
$\Delta_h(5, 6)$	15.0	12	18	17.1	16.1	15.3	14.4	15.5	13.7

TABLE II. First hole Coulomb energy J_{ss} and single-particle energy level spacings in meV, from atomistic pseudopotential calculations for six different self-assembled len-shaped InAs/GaAs quantum dots. All sizes are in nm.

	$2R = 20$		$2R = 25$		$2R = 27.5$	
	$h = 2.5$	$h = 3.5$	$h = 2.5$	$h = 3.5$	$h = 2.5$	$h = 3.5$
J_{ss}	27.2	22.1	25.1	20.4	24.2	19.6
$\delta_{p1,p2}$	10.9	11.3	7.1	9.5	5.8	7.9
$\delta_{p2,d1}$	4.5	3.4	8.3	2.4	9.4	3.9

tained for the InAs dot with 20 nm base and 2.5 nm height, with differences in the addition energies of less than 16%, compared with almost 50% error in 2D-EMA model (despite the fact that two of the addition energies were fitted in the later case). The parameters $\delta_{p1,p2}$ and $\delta_{p2,d1}$ calculated for different dots are given in Table II and, as shown in Fig. 1(c) (right side), lie close to the center of the predicted phases $^1\Delta$, $^2\Delta$ and $^1\Sigma^*$. This indicates the stability of the numerical results against possible variations of $\delta_{p1,p2}$ and $\delta_{p2,d1}$ due to shape anisotropy or alloy effects.

The predicted charging pattern [Fig. 1(c) (left side)] shows that the level filling by holes does not follow the Aufbau principle nor the Hund's rules: d levels get filled before the second p level, despite the fact that the d level is energetically more than 3 meV above the second p level [26]. The nontrivial hole filling pattern is due to two reasons. First, the large p-level splitting leads to the p_2 level being energetically close to the d_1 level; i.e., δ_{p_2,d_1} is small. In Table II, we list the hole single-particle energy spacings and the first hole Coulomb integrals J_{ss} for different dots. We see that $\delta_{p_1,p_2} \sim (0.3 - 0.5)J_{ss}$ and $\delta_{p_2,d_1} \sim (0.2 - 0.3)J_{ss}$, which differ significantly from the assumption of 2D-EMA models where $\delta_{p1,p2} \sim 0$, and $\delta_{p2,d1} \sim J_{ss}$. Second, the Coulomb repulsion between the p_1 and the d level is lower than that between the two p levels, therefore the Coulomb energy can overcome the single-particle energy spacing δ_{p_2,d_1}, leading to the non-Aufbau charging pattern.

An important feature of the present theory is not only its compatibility with the zero field experimental results but also with the magnetic field dependence obtained in Ref. [15]. In our calculations, the hole single-particle level p_1 has mixed characters of $L_z = +1$ and $L_z = -1$. This state which is Kramers degenerate at $B = 0$ will therefore split in opposite direction in the magnetic field. This agrees with the observation of the hole charging experiment [15]. This is also true for p_2, which has both $L_z = +1$ and $L_z = -1$ characters and d_1, d_2, which have $L_z = +2$ and $L_z = -2$ characters.

In conclusion, we developed a general phase-diagram approach that classifies the many-particle configurations for electrons and holes in quantum dots in terms of simple electronic and geometric parameters. From these diagrams, we predict that the hole charging sequence presents surprising configurations (unexpected from effective mass model) that violates the Aufbau principle as well as the Hund's rule. Our results are in good agreement with recent experimental findings and provide a novel way to study the charging of carriers in quantum dots.

This work was supported by US DOE-SC-BES-DMS, under NREL Contract No. DEAC36-99-GO10337.

[1] H. Drexler *et al.*, Phys. Rev. Lett. **73**, 2252 (1994).
[2] M. C. Bödefeld *et al.*, Appl. Phys. Lett. **74**, 1839 (1999).
[3] D. V. Regelman *et al.*, Phys. Rev. B **64**, 165301 (2001).
[4] S. Tarucha *et al.*, Phys. Rev. Lett. **77**, 3613 (1996).
[5] L. P. Kouwenhoven *et al.*, Science **278**, 1788 (1997).
[6] M. Kastner, Phys. Today **46** No. 1, 24 (1993).
[7] C. H. Bennett *et al.*, Nature (London) **404**, 247 (2000).
[8] A. Imamoglu *et al.*, Phys. Rev. Lett. **83**, 4204 (1999).
[9] G. Yusa and H. Sakaki, Appl. Phys. Lett. **70**, 345 (1997).
[10] M. Kroutvar *et al.*, Appl. Phys. Lett. **83**, 443 (2003).
[11] P. Michler *et al.*, Science **290**, 2282 (2000).
[12] U. Banin *et al.*, J. Chem. Phys. **109**, 2306 (1998).
[13] J. J. Finley *et al.*, Phys. Rev. B **63**, 073307 (2001).
[14] D. Reuter *et al.*, Physica (Amsterdam) **21E**, 445 (2004).
[15] D. Reuter *et al.*, Phys. Rev. Lett. **94**, 026808 (2005).
[16] A. J. Williamson *et al.*, Phys. Rev. B **62**, 12 963 (2000).
[17] A. Franceschetti *et al.*, Phys. Rev. B **60**, 1819 (1999).
[18] L. Jacak, P. Hawrylak, and A. Wójs, *Quantum Dots* (Springer-Verlag, Berlin, 1998).
[19] R. J. Warburton *et al.*, Phys. Rev. B **58**, 16 221 (1998).
[20] Note that the term "spin" for holes is not an actual electronic spin, but rather a index for two Kramers degenerate states. Thus, the exchange integrals $K_{i\sigma,j\sigma'}$ are not simply diagonal in σ, σ' as in Eq. (1) which is widely used in the literature [19]. We used in our calculations the full exchange matrix.
[21] Indeed, there are indications that the p levels and the d levels of self-assembled quantum dots are, in fact, split. This is known from multiexcitons measurements [3] as well as from our theoretical analysis [22], showing that the underlying zinc-blende symmetry induces such splitting $\epsilon_{p_1} \neq \epsilon_{p_2}$ and $\epsilon_{d_1} \neq \epsilon_{d_2}$, even for cylindrically symmetric dots.
[22] G. Bester *et al.*, Phys. Rev. B **71**, 045318 (2005).
[23] T. Walther *et al.*, Phys. Rev. Lett. **86**, 2381 (2001).
[24] L. He *et al.*, Phys. Rev. B **70**, 235316 (2004).
[25] For example, the first 3 electron and hole wave functions of lens-shaped InAs/GaAs quantum dots with base $2R = 25$ nm and height $h = 3.5$ nm are plotted in Ref. [24], where the projection of wave functions into angular momentum are listed in Table II of Ref. [24]. As can be seen both electron and holes states are not pure s or p unlike what is assumed in the 2D-EMA model. Here we use the leading projections to label the single-particle states. Similarly, the S and Λ in Eqs. (2)–(4) are used for the purpose of notations only, and are not the real total spin and total angular momentum of the many-particle hole states.
[26] The violation of the Aufbau principle implies here that the order of level occupation in the *total* (CI) energies is different from the order of levels in the underlying single-particle pseudopotential calculations. Such violation need not occur when CI is compared with Hartree-Fock.